Clinical Interventions in Aging

Dovepress
Taylor & Francis Group

Open Access Full Text Article

ORIGINAL RESEARCH

Multi-Omics Reveals Dysregulation of the Endosome-Lysosome-Autophagy Axis and Immune-Inflammatory Imbalance in Elderly Sepsis

Yi Gou, Ziyu Xia, Nazila Haireti, Ailikuti Aikepaer, Jianzhong Yang, Dandan Li

Emergency Trauma Center, The First Affiliated Hospital of Xinjiang Medical University, Urumqi, People's Republic of China

Correspondence: Dandan Li; Jianzhong Yang, Emergency Trauma Center, The First Affiliated Hospital of Xinjiang Medical University, Urumqi, People's Republic of China, Email 54327011O@qq.com; yjz6542@126.com

Background: Elderly sepsis (ES), characterized by dual insults of aging and sepsis, is associated with substantial morbidity and mortality and exhibits distinct pathophysiological features. Elucidating these unique mechanisms is critical for developing precise therapeutic strategies and improving patient prognoses.

Methods: We performed integrative analyses of untargeted metabolomics and proteomics in four groups: young and elderly healthy controls and young and elderly patients with sepsis. Characteristic metabolites and proteins in ES were identified by using a three-step screening pipeline. Pairwise correlation analyses were conducted on the screened molecules; those with a $|r_s| \geq 0.4$ were retained for subsequent KEGG and/or GO functional enrichment analyses.

Results: Two characteristic metabolites and seven proteins were identified: D-aspartic acid, LysoPC (18:1/0:0), SCGB3A2, ATP6V1E1, APOA1, AP1G1, INHBC, CRYZL1, and CXCL14. Enriched metabolic pathways comprised D-Amino acid metabolism, alanine, aspartate, and glutamate metabolism, and glycerophospholipid metabolism. Enriched protein-centric functional terms were linked to the endocytic vesicle lumen, proton-translocating V-type ATPase, receptor ligand activity, and signaling receptor activator activity, etc. Collectively, these findings highlight perturbations in the endosome–lysosome–autophagy axis and immune-inflammatory imbalance in ES.

Conclusion: This study established a hypothesis implicating dysregulation of the endosome-lysosome-autophagy axis and immune-inflammatory imbalance in ES, thus providing a theoretical foundation for further elucidating the pathophysiological mechanisms underlying ES and developing precise therapeutic interventions.

Keywords: elderly sepsis, multi-omics, untargeted metabolomics, proteomics

Introduction

Sepsis, defined as life-threatening organ dysfunction resulting from a dysregulated host response to infection, remains a leading cause of global morbidity and mortality.[1,2] Owing to immunosenescence, comorbidities, impaired physiological function, frailty, and reduced organ reserve, elderly individuals are not only more susceptible to sepsis but also experience significantly poorer outcomes.[3,4] Elderly sepsis (ES) accounts for a disproportionately large proportion of all sepsis cases (approximately 60–85%), and this proportion is projected to rise further with the progression of global population aging.[5] ES has emerged as a key focus for emergency and critical care physicians. Extensive research has focused on ES risk stratification to facilitate early identification and intervention in high-risk patients.[5–7] Nevertheless, risk stratification alone is insufficient to underpin the development of personalized precision therapies for ES. Owing to the synergistic effects of senescence and sepsis, the pathophysiological features of ES may differ from those in younger adults with sepsis. Elucidating the unique pathophysiological alterations associated with sepsis in the elderly is a prerequisite for advancing precision and personalized therapies. However, the current understanding of the pathophysiological characteristics of sepsis in the elderly population remains limited.

https://doi.org/10.2147/CIA.S613629
Received: 1 April 2026
Accepted: 18 May 2026
Published: 26 May 2026

Using a murine cecal ligation and puncture (CLP) polymicrobial sepsis model, Lin et al[8] employed single-cell RNA sequencing (scRNA-seq) to demonstrate that monocytes and macrophages from aged septic mice exhibited a hyperinflammatory yet functionally exhausted phenotype, with both monocytes and dendritic cells displaying impaired antigen-presenting capacity. This study offers critical insights into immune remodeling in ES. Notably, although the CLP model recapitulates polymicrobial sepsis, the inherent discrepancies between murine models and clinical sepsis limit the translational relevance of these findings. Addressing the limitations of prior studies, He et al[3] leveraged peripheral blood samples from ES patients, younger patients with sepsis, and healthy controls to construct a single-cell atlas of immunological landscapes. They further identified that innate immune cells in ES exhibit hyperinflammatory and senescent phenotypes along with a compromised antigen-presenting function. Focusing on immune pathways, these studies provide key insights into the immunological response profile of ES. Nevertheless, reliance solely on scRNA-seq provides limited utility for deciphering comprehensive pathophysiological alterations underlying ES.

Systems biology, encompassing genomics, transcriptomics, proteomics, and metabolomics, has emerged as a robust tool for comprehensively deciphering the pathophysiological characteristics of diseases.[9–12] Multiomics studies enable cross-layer validation and integrated multilevel investigations (genetic, transcriptional, proteomic, and metabolic), facilitating a more thorough delineation of disease pathophysiological mechanisms.[13] By integrating metabolomic and transcriptomic profiling, Xu et al[10] identified marked perturbations in energy metabolism, arginine and tyrosine metabolism, inflammation, and oxidative stress in ES. However, by comparing ES patients with healthy elderly controls, this study revealed pathophysiological disturbances in ES, but failed to disentangle the contributions of natural senescence from those of sepsis. Thus, the unique pathophysiological alterations specific to ES remain unclear.

Therefore, we integrated untargeted metabolomics and proteomics, and employed multiple intergroup comparisons to dissect the unique pathophysiological characteristics specific to ES. Initially, we compared ES patients with elderly healthy controls (EHCs) to identify ES-associated pathophysiological perturbations. Next, we excluded differential molecules (metabolites and proteins) overlapping with those identified from the comparison between young sepsis (YS) patients and young healthy controls (YHCs) to rule out the general effects of sepsis per se. Subsequently, we removed the differential molecules overlapping with those derived from EHCs and YHCs to eliminate the confounding influence of natural senescence. Finally, the remaining differential molecules common to the ES vs. YS comparison were defined as the ES-specific hallmark molecules. Pathway enrichment analysis was performed to delineate the pathophysiological mechanisms underlying ES. To our knowledge, no prior study has integrated metabolomics and proteomics to uncover the hallmark pathophysiological features of ES, and few studies have utilized this innovative multi-tiered screening strategy for comprehensive exploration of its pathophysiological perturbations. By leveraging these innovations, this study offers insights into the unique pathophysiological characteristics of ES.

Methods

Ethnics Statement

This study was conducted in accordance with the ethical principles stated in the 1964 Declaration of Helsinki and its later amendments, and was approved by the Medical Ethics Committee of the First Affiliated Hospital of Xinjiang Medical University (20251215–33). As the present study used existing metabolomic and proteomic data, the requirement for informed consent was waived. To protect patient privacy, all personally identifiable information was de-identified, and data were analyzed in anonymized form by the research team only.

Study Design and Patient Selection

A total of 74 participants comprising sepsis patients and healthy controls, were enrolled at the First Affiliated Hospital of Xinjiang Medical University between March 2023 and November 2024. The cohort included 23 ES patients (≥65 years), 31 YS patients (20–64 years), 11 EHCs (≥65 years), and 9 YHCs (20–64 years). Sepsis was diagnosed in accordance with the Sepsis-3 criteria,[1] defined as a confirmed infection plus a Sequential Organ Failure Assessment (SOFA) score ≥ 2. The inclusion criteria were as follows: 1) fulfillment of the Sepsis-3 diagnostic criteria and 2) age ≥18 years. Exclusion criteria were as follows: 1) pregnant or lactating females; 2) patients with immunodeficiency, receiving immunotherapy, or with malignant tumors; 3) patients with traumatic sepsis; and 4) patients with pre-existing severe dysfunction of the liver, kidneys, heart, or lungs.

Our strategy and workflow for identifying ES-specific pathophysiological signatures are outlined in the Introduction and illustrated in Figure 1. At the time of blood sampling, all healthy volunteers were free of infectious, autoimmune, or malignant diseases. Peripheral venous blood was collected in EDTA-K_2 anticoagulant tubes within 1 hour after sepsis patients were admitted to the emergency resuscitation area. Within 10 min of collection, the samples were centrifuged at 3000 × g for 10 min at room temperature to isolate plasma, which was then stored at −80 °C. Detailed metabolomic and proteomic analyses are provided in Supplementary Material 1.

Data Collection

Clinical data, including age, sex, disease severity scores, comorbidities, vital signs, blood glucose, albumin, lactate, complete blood count parameters, and inflammatory markers, were extracted from electronic medical records.

Statistical Analysis

Statistical analyses of the clinical data were performed using IBM SPSS Statistics (version 26.0). Normality of data distribution was assessed using the Kolmogorov–Smirnov test. Normally distributed continuous variables were expressed as mean ± standard deviation and compared across groups using the independent-samples *t*-test. Non-normally distributed variables are presented as medians (interquartile range, Q1–Q3), with between-group comparisons conducted using the Mann–Whitney *U*-test. Categorical variables are summarized as counts (percentages), and intergroup differences were analyzed using Pearson's χ^2 test, Fisher's exact test, or the continuity-corrected χ^2 test. Statistical significance was set at $P < 0.05$.

Proteins with >40% missing values were excluded, whereas those with <40% missing values were imputed using a probabilistic principal component analysis. Before statistical testing, metabolomic and proteomic data were $\log_{10}$-transformed and autoscaled to ensure comparability across metabolites and proteins with divergent abundance levels. Partial least squares discriminant analysis (PLS-DA) was performed to compute variable importance in projection (VIP) scores and assess the discriminatory power of omics profiles with a permutation test applied to evaluate the potential overfitting of the PLS-DA model. The P-value was derived from the *t*-test, and fold-change (FC) values were calculated using FC analysis. Differentially expressed metabolites (DEMs) were defined as features with $P < 0.05$, and VIP > 1. Differentially expressed proteins (DEPs) were identified using thresholds of $P < 0.05$, FC > 1.5 (upregulated) or FC < 0.67 (downregulated). Kyoto Encyclopedia of Genes and Genomes (KEGG) and Gene Ontology (GO) enrichment analyses were performed for the DEMs and DEPs. PLS-DA, FC analysis, heatmap construction (Euclidean distance and *t*-test), DEM pathway enrichment, and correlation analysis were performed using the MetaboAnalyst 6.0 (https://www.metaboanalyst.ca/). Volcano plots, Sankey bubble plots, Venn diagrams, DEP functional enrichment analysis, and correlation coefficient networks were generated using Wei Sheng Xing Bioinformatics Platform (https://bioinformatics.com.cn/). Violin and linear correlation plots were constructed using GraphPad Prism v8.3.0.

Results

Clinical Characteristics

As shown in Table 1, no significant between-group differences were observed in sex, disease severity score, or the prevalence of diabetes and coronary heart disease between the ES and YS groups (all $P > 0.05$). However, the ES group exhibited a significantly higher prevalence of hypertension and markedly lower ANC and AMC than the YS group. Similarly, no significant differences in sex or prevalence of hypertension and diabetes were detected in the comparisons of ES versus EHC (Supplementary 2: STable 1), YS versus YHC (Supplementary 2: STable 2), and EHC versus YHC (Supplementary 2: STable 3).

Unraveling the Characteristic Pathophysiological Alterations of Sepsis in the Elderly via Metabolomics

Partial Least Squares Discriminant Analysis

We developed a PLS-DA model based on metabolomic profiles to dissect the independent and combined effects of ageing and sepsis. PLS-DA score plots showed a clear separation between septic patients and healthy controls in both the

https://doi.org/10.2147/CIA.S613629

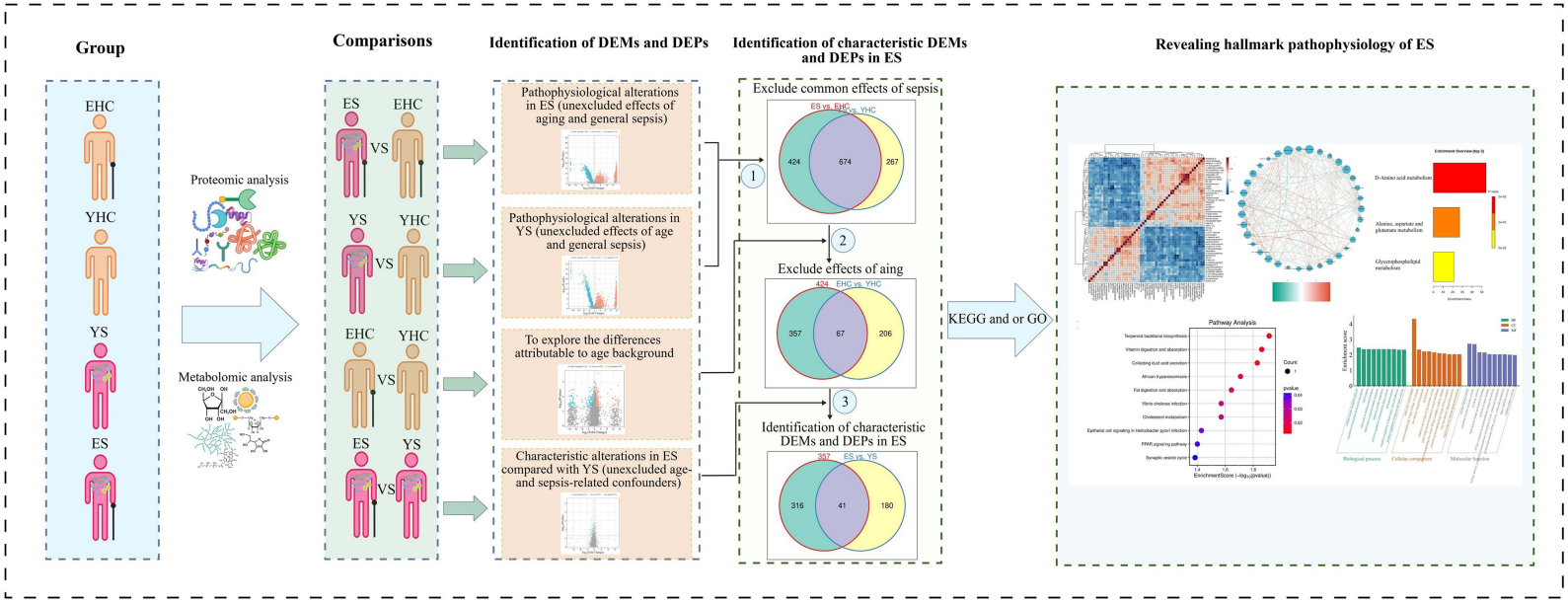

Figure 1 Study design diagram. Note: Created with BioGDP.com.[14] ①Initially, we compared ES patients with EHCs to initially pinpoint ES-associated pathophysiological perturbations. Next, we excluded differential molecules (metabolites and proteins) overlapping with those identified from the comparison of YS patients vs. YHCs, to rule out the general effects of sepsis per se; ② Among the 424 signature molecules identified in the primary screening, several were influenced by natural aging (EHC vs. YHC). We removed these overlapping molecules associated with natural aging to rule out its confounding effects; ③Among the 221 DEMs and DEPs identified in ES versus YS, 41 overlapped with the 357 signature molecules screened in the first and second screening steps. These overlapping molecules were defined as the signature factors of aged sepsis.

Abbreviations: EHC, elderly healthy control; YHC, young healthy control; YS, young sepsis; ES, elderly sepsis; DEMs, differentially expressed metabolites; DEPs, differentially expressed proteins; KEGG, Kyoto Encyclopedia of Genes and Genomes; GO, Gene Ontology.

Table 1 A Comparison of the Clinical Characteristics of ES and YS Groups

Clinical Characteristics	YS (N=31)	ES (N=23)	χ^2/t/Z	*P*-value
Age (years old)	52.1±10.9	73.1±6.0	−8.297	<0.001
Male (n, %)	24 (77.4)	15 (65.2)	0.980	0.322
Disease severity score				
SOFA (score)	4.0 (2.0, 5.3)	4.5 (2.2, 5.8)	−0.313	0.755
APACHE-II (score)	15.9±7.9	16.3±4.3	−0.237	0.814
GCS (score)	14.0 (12.0, 15.0)	15.0 (14.0, 15.0)	−1.557	0.120
Comorbidity (n, %)				
Hypertension	10 (32.3)	14 (60.9)	4.378	0.036
Diabetes	6 (19.4)	6 (26.1)	0.346	0.556
Coronary heart disease	8 (25.8)	8 (34.8)	0.510	0.475
Vital signs				
MAP (mmHg)	81.3±22.5	86.8±19.4	−0.934	0.355
Heart rate (times/min)	120.0±21.4	116.8±23.6	0.516	0.608
Respiratory rate (times/min)	26.9±5.8	27.1±5.4	−0.168	0.867
Glucose (mmol/L)	7.5 (5.4, 12.1)	7.9 (6.0, 11.3)	−0.175	0.861
Albumin (g/L)	30.4±5.6	33.1±4.5	−1.828	0.073
Lactic acid (mmol/L)	3.3 (2.3, 7.0)	2.9 (2.2, 4.0)	−1.190	0.234
Complete blood count				
ANC (10^3/mm^3)	10.6 (6.9, 16.9)	8.3 (2.0, 11.2)	−2.265	0.023
ALC (10^3/mm^3)	0.6 (0.5, 1.3)	0.5 (0.3, 0.9)	−1.723	0.085
AMC (10^3/mm^3)	0.7 (0.4, 1.2)	0.3 (0.2, 0.6)	−3.202	0.001
Hemoglobin (g/L)	121.4±39.7	106.35±31.8	1.491	0.142
Inflammatory markers				
CRP (mg/L)	90.0 (54.7, 90.0)	90.0 (68.0, 90.0)	−1.403	0.161
IL-6 (pg/mL)	217.0 (74.7, 3438.0)	709.0 (49.5, 5000.0)	−0.203	0.839
Procalcitonin (ng/mL)	13.0 (3.2, 82.8)	3.2 (0.4, 28.6)	−1.916	0.055
SAA (mg/L)	245.0 (166.0, 259.5)	251.4 (141.3, 2271.8)	−0.866	0.387

Abbreviations: ES, elderly sepsis; YS, young sepsis; SOFA, sequential organ Failure assessment; APACHE-II= acute physiology and chronic health evaluation II; GCS, Glasgow Coma Scale; MAP, mean arterial pressure; ANC, absolute neutrophil count; ALC, absolute lymphocyte count; AMC=absolute monocyte count; CRP, C-reactive protein; IL-6, interleukin-6; SAA, serum amyloid A.

elderly (ES vs. EHC) and young (YS vs. YHC) cohorts, indicating that sepsis elicits substantial pathophysiological perturbations (Figure 2A). Distinct clustering was also observed between EHC and YHC groups, suggesting that age alone served as a strong discriminator. Most importantly, the PLS-DA model effectively distinguished ES from YS, demonstrating that aging imparts a unique molecular signature for septic stress (Figure 2A). Cross-validation confirmed that the model achieved favorable discriminatory performance with four principal components (accuracy = 0.7072, R^2 = 0.9387, Q^2 = 0.4301) (Figure 2B). Permutation testing further demonstrated that all performance metrics of the original model were significantly higher than the corresponding values under random permutation, supporting the statistical reliability of the model and excluding overfitting (Figure 2C).

Identification of Differential Metabolites

A total of 1098 DEMs were identified in the ES versus EHC comparison, including 418 upregulated and 680 downregulated features (Figure 3A). Correspondingly, 941, 273, and 221 DEMs were detected in the YS versus YHC (Figure 3B), EHC versus YHC (Figure 3C), and ES versus YS (Figure 3D) comparisons, respectively. Heatmaps based on the top 25 DEMs for each contrast yielded clear separation between the respective groups: ES versus EHC (Figure 3E), YS versus YHC (Figure 3F), EHC versus YHC (Figure 3G), and ES versus YS (Figure 3H).

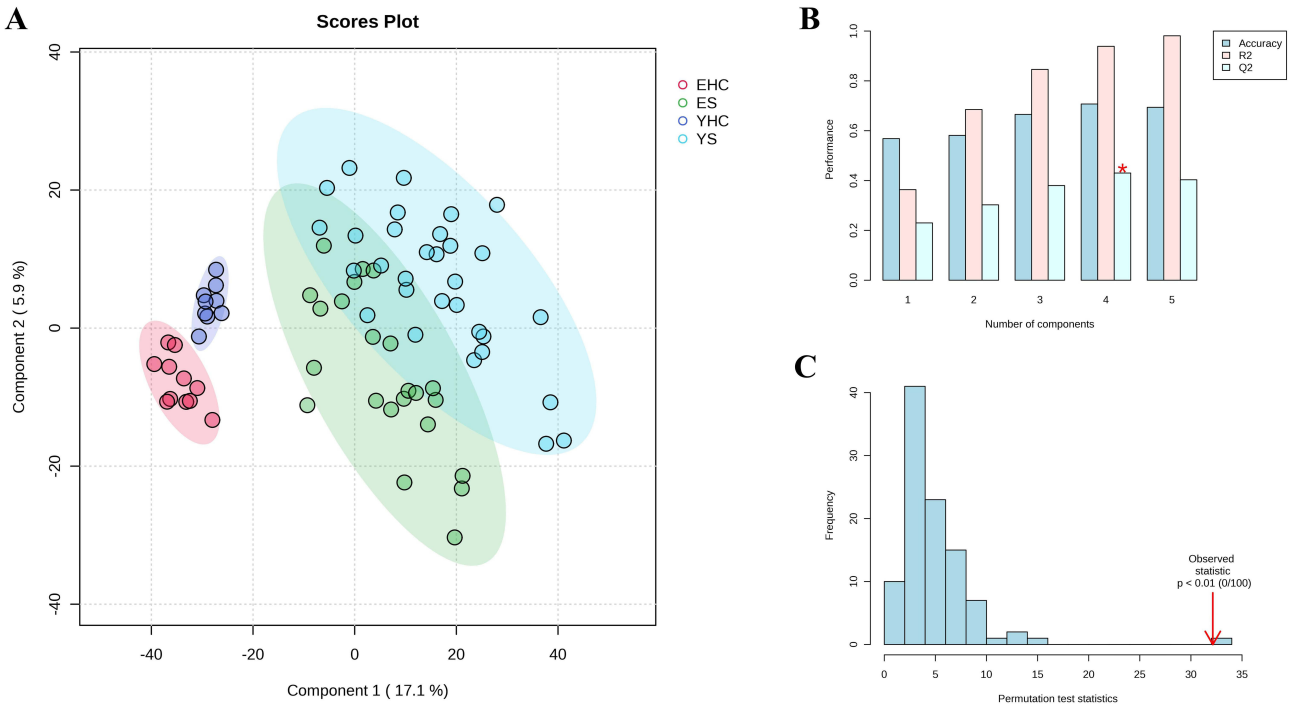

Figure 2 PLS-DA. (**A**) PLS-DA score plots; (**B**) Principal component selection; (**C**) Permutation test. R^2 represents the proportion of variance in the response variable Y explained by the model; the closer the R^2 value is to 1, the better the model fits the categorical differences of samples in the training set, and the more distinct the intergroup separation. Q^2 reflects the predictive ability of the model; a Q^2 value closer to 1 indicates better model predictive performance. ★ Selected principal component based on the largest Q^2.
Abbreviation: PLS-DA, Partial least squares discriminant analysis.

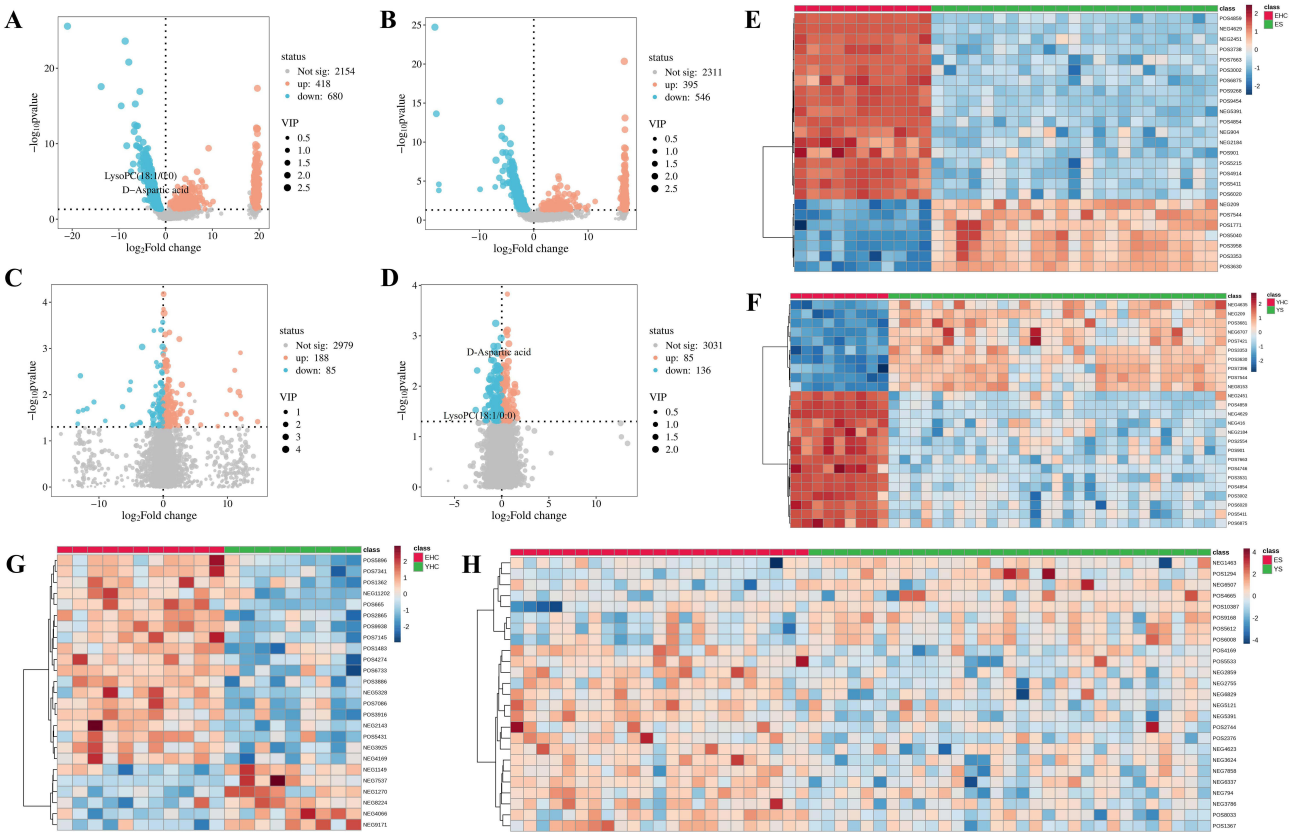

Figure 3 Volcano plot and Heatmap in metabolomics. (**A**) Volcano plot in ES vs. EHC; (**B**) Volcano plot in YS vs. YHC; (**C**) Volcano plot in EHC vs. YHC; (**D**) Volcano plot in ES vs. YS; (**E**) Heatmap in ES vs. EHC; (**F**) Heatmap in YS vs. YHC; (**G**) Heatmap in EHC vs. YHC; (**H**) Heatmap in ES vs. YS.
Abbreviations: VIP, variable importance in projection; EHC, elderly healthy control; YHC, young healthy control; YS, young sepsis; ES, elderly sepsis.

https://doi.org/10.2147/CIA.S613629

Enrichment Analysis of Differential Metabolites

KEGG pathway enrichment analysis was performed across four pairwise comparisons to dissect metabolic alterations linked to sepsis and aging (Figure 4A–D, corresponding to ES vs. EHC, YS vs. YHC, EHC vs. YHC, and ES vs. YS, respectively). To visualize the shared and age-specific metabolic perturbations induced by sepsis, we constructed a pathway co-enrichment network between ES patients (ES vs. EHC) and young sepsis patients (YS vs. YHC) (Figure 4E).

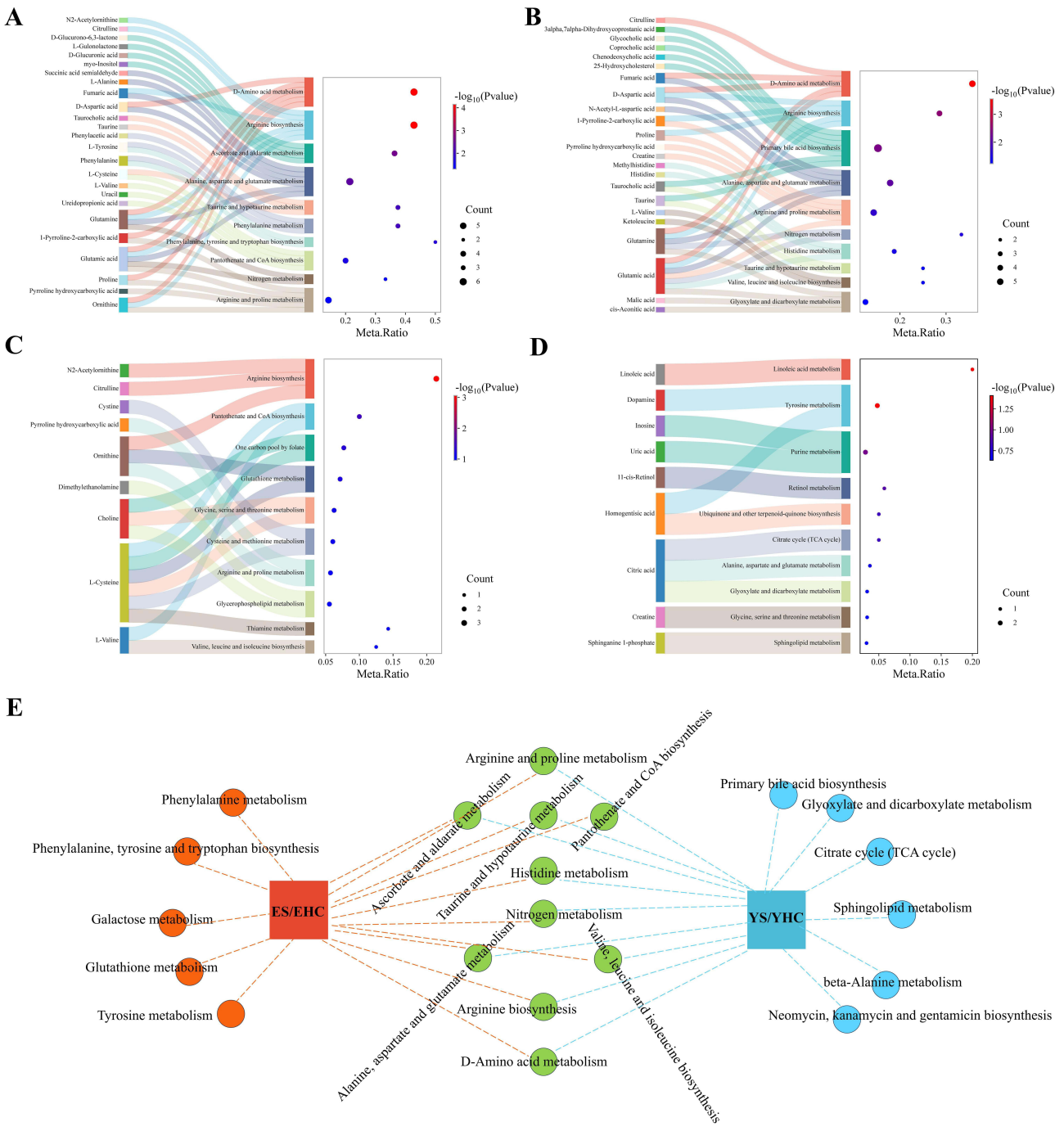

Figure 4 KEGG Enrichment analysis. (**A**) Top 10 metabolic pathways and enriched metabolites in ES vs. EHC; (**B**) Top 10 metabolic pathways and enriched metabolites in YS vs. YHC; (**C**) Top 10 metabolic pathways and enriched metabolites in EHC vs. YHC; (**D**) Top 10 metabolic pathways and enriched metabolites in ES vs. YS; (**E**). Co-enrichment network between elderly sepsis (ES vs. EHC) and young sepsis (YS vs. YHC).

https://doi.org/10.2147/CIA.S613629

Conserved Metabolic Signatures of Sepsis

ES vs. EHC and YS vs. YHC exhibited a significant overlap in core metabolic pathways, indicating a universal septic response across age groups. These shared enriched pathways included 1) amino acid metabolic networks: arginine biosynthesis, arginine and proline metabolism, alanine, aspartate, and glutamate metabolism; taurine and hypotaurine metabolism; histidine metabolism; d-amino acid metabolism; and valine, leucine, and isoleucine biosynthesis; 2) nitrogen and cofactor metabolism, nitrogen metabolism, and pantothenate and CoA biosynthesis; and 3) antioxidant-related carbohydrate metabolism, ascorbate, and aldarate metabolism. This overlap highlights that sepsis universally disrupts amino acid catabolism, nitrogen homeostasis, branched-chain amino acid anabolism, cofactor biosynthesis, and redox-related carbohydrate metabolism regardless of patient age.

Age-Specific Metabolic Perturbations in Sepsis

Distinct pathway enrichment emerged between the elderly and young patients with sepsis, reflecting divergent pathophysiological responses.

Specific Pathways in ES (ES vs. EHC)

Unique enrichment was detected in aromatic amino acid metabolism (phenylalanine metabolism and phenylalanine, tyrosine, and tryptophan biosynthesis), carbohydrate metabolism (galactose metabolism), redox regulation (glutathione metabolism), and tyrosine metabolism. These findings suggest that ES is characterized by disrupted aromatic amino acid homeostasis, impaired antioxidant defenses, and altered carbohydrate metabolism.

Specific Pathways in YS (YS vs. YHC)

Exclusive enrichment was identified in energy metabolism (citrate cycle (TCA cycle), glyoxylate and dicarboxylate metabolism), lipid signaling (sphingolipid metabolism), bile acid homeostasis (primary bile acid biosynthesis), beta-alanine metabolism, and secondary metabolite biosynthesis (neomycin, kanamycin, and gentamicin biosynthesis). This profile indicated that sepsis in young patients preferentially affects mitochondrial energy metabolism, lipid-mediated inflammatory signaling, and bile acid metabolism, reflecting distinct metabolic stress adaptations in younger patients.

Baseline Metabolic Perturbations Associated with Healthy Aging (EHC vs. YHC)

Figure 4C depicts age-related metabolic changes and identifies core pathways, including amino acid metabolism (arginine biosynthesis, arginine and proline metabolism, glycine, serine and threonine metabolism, and cysteine and methionine metabolism), one-carbon metabolism (one carbon pool by folate), metabolic dysregulation of redox- and energy-related cofactors (glutathione metabolism, pantothenate and CoA biosynthesis, and thiamine metabolism), and membrane lipid remodeling (glycerophospholipid metabolism). These pre-existing metabolic differences provide a critical context for interpreting age-divergent metabolic responses in sepsis, where aging may exacerbate septic stress-induced metabolic dysregulation in elderly patients.

Characteristic Metabolic Disturbances in Elderly Sepsis

We identified 41 ES-specific DEMs via four pairwise comparisons: ES vs. EHC, YS vs. YHC, EHC vs. YHC, and ES vs. YS (Figure 5A). KEGG pathway enrichment analysis of these 41 ES-specific DEMs identified four significantly enriched pathways: d-amino acid metabolism; alanine, aspartate, and glutamate metabolism; glycerophospholipid metabolism; and tryptophan metabolism (Figure 5B). Pathway enrichment was primarily driven by three core metabolites, 2-aminobenzoic acid, LysoPC (18:1/0:0), and D-aspartic acid. These three metabolites showed progressively decreasing trends across the EHC, YHC, YS, and ES cohorts (Figure 5C). Positive correlations were detected between LysoPC (18:1/0:0) and D-aspartic acid and between 2-aminobenzoic acid and D-aspartic acid (Figure 5D). Collectively, these findings delineate the unique metabolic signature of ES, characterized by dysregulated d-amino acid metabolism, perturbed glycerophospholipid homeostasis, and altered tryptophan catabolism, thereby offering novel insights into the pathophysiological vulnerabilities of elderly patients during septic insults.

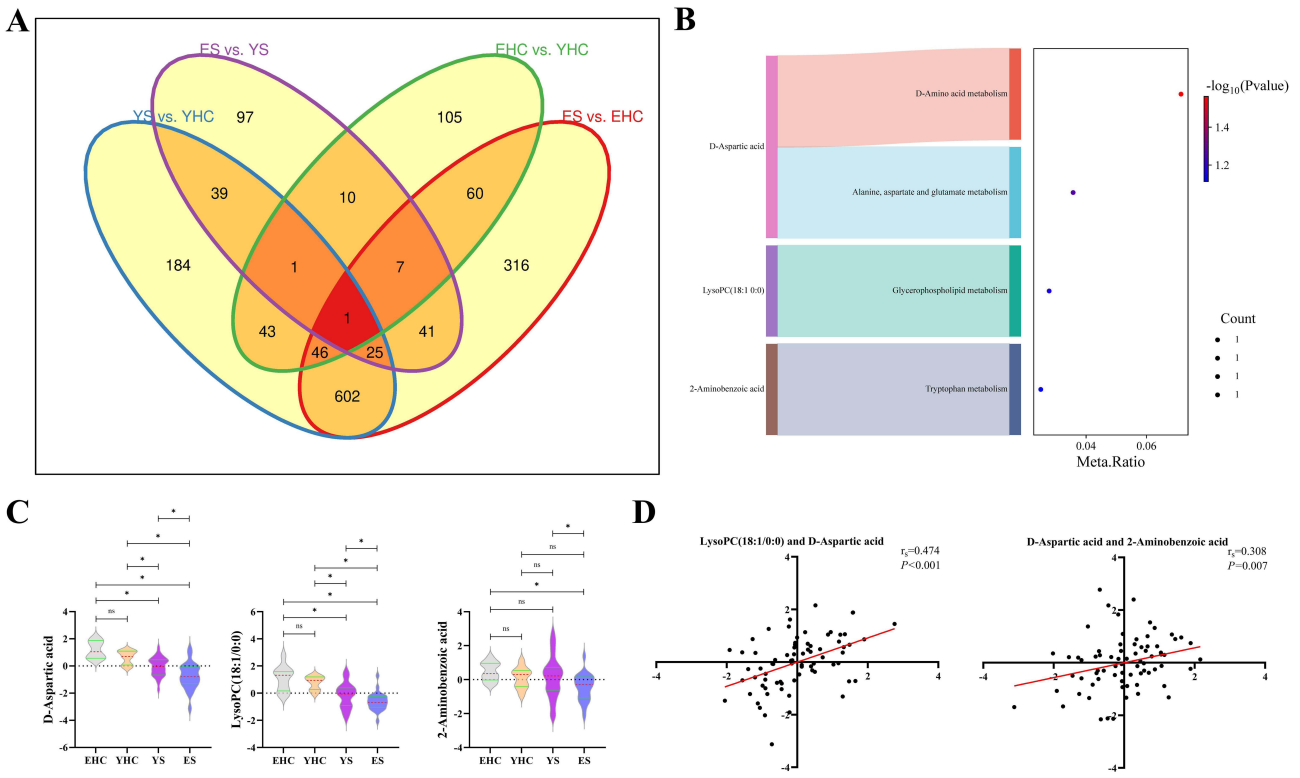

Figure 5 Characteristic Metabolic Disturbances in Elderly Sepsis. (**A**) Identification of differential metabolites specific to elderly sepsis; (**B**) KEGG enrichment analysis of differential metabolites specific to elderly sepsis; (**C**) The levels of D-aspartic acid, LysoPC (18:1/0:0), and 2-Aminobenzoic acid in EHC, YHC, YS, and ES groups; (**D**) correlations between LysoPC(18:1/0:0) and D-aspartic acid, as well as between 2-aminobenzoic acid and D-aspartic acid. *Statistically significant difference (P<0.05).
Abbreviations: EHC, elderly healthy control; YHC, young healthy control; YS, young sepsis; ES, elderly sepsis; ns, not significant.

Unraveling the Characteristic Pathophysiological Alterations of Sepsis in the Elderly via Proteomics

Similarly, a PLS-DA model, constructed using proteomic data, was used to investigate the distinct and interactive effects of age and sepsis. PLS-DA score plots demonstrated that the model could effectively discriminate ES from EHC, YS from YHC, EHC from YHC, and ES from YS (Figure 6A). Cross-validation revealed that the model exhibited a favorable discriminatory ability for the five principal components (accuracy = 0.6977, R^2 = 0.9544, Q^2 = 0.3597) (Figure 6B). The permutation test suggested that the model was statistically reliable without overfitting (Figure 6C).

Identification of Differentially Expressed Proteins

A total of 2702 DEPs were identified in the ES vs. EHC comparison, among which 1176 were upregulated and 1526 were downregulated (Figure 7A). Similarly, 2419, 380, and 105 DEPs were identified in the YS vs. YHC (Figure 7B), EHC vs. YHC (Figure 7C), and ES vs. YS (Figure 7D) comparisons, respectively. The heatmaps constructed using these DEPs (top 25) clearly distinguished between different groups, including ES vs. EHC (Figure 7E), YS vs. YHC (Figure 7F), EHC vs. YHC (Figure 7G), and ES vs. YS (Figure 7H).

KEGG Enrichment Analysis of Differentially Expressed Proteins

To characterize the proteomic perturbations underlying sepsis and age-dependent heterogeneity, we performed KEGG pathway enrichment analysis of the DEPs (Figure 8A–D. Given the large number of enriched pathways, we focused on the top five shared pathways (common to both ES vs. EHC and YS vs. YHC), top five pathways specific to ES vs. EHC, and top five pathways specific to YS vs. YHC (Figure 8E). This proteomic pathway analysis identified core septic response pathways shared across age groups while revealing distinct age-specific proteomic signatures.

https://doi.org/10.2147/CIA.S613629

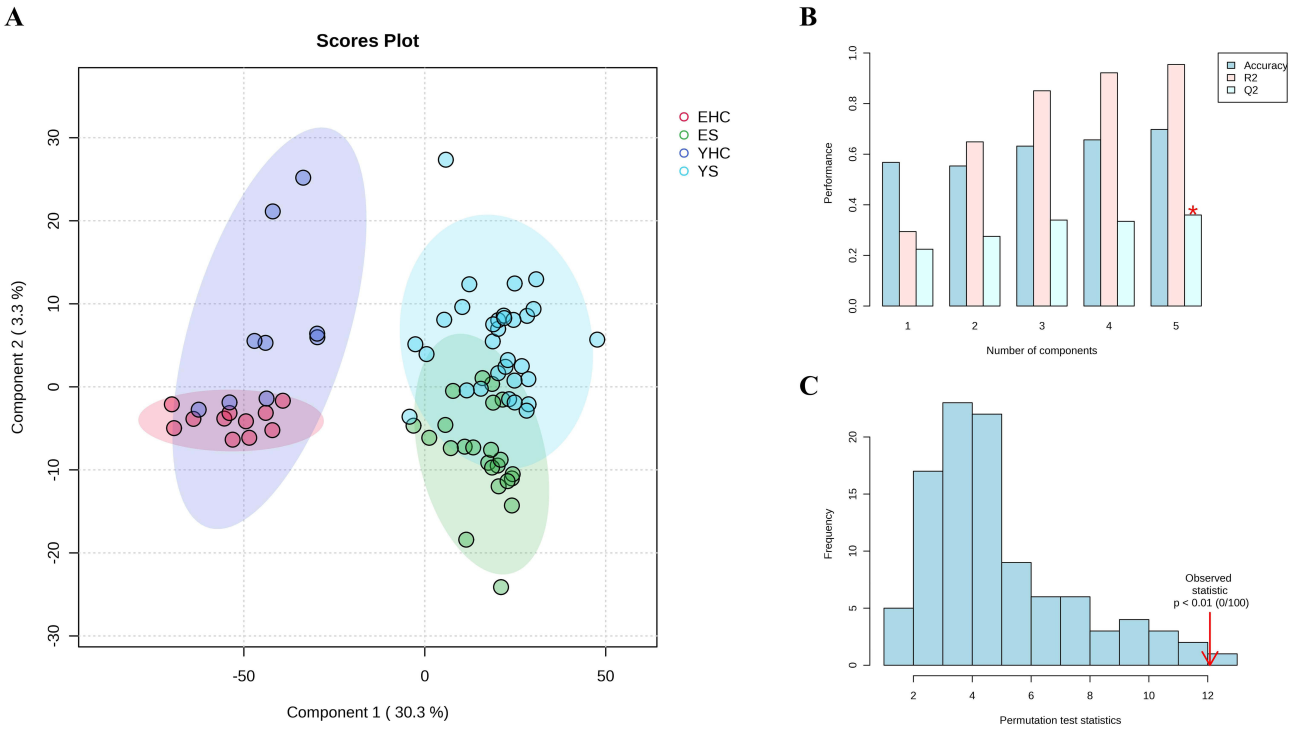

Figure 6 PLS-DA. (**A**) PLS-DA score plots; (**B**) Principal component selection; (**C**) Permutation test. R^2 represents the proportion of variance in the response variable Y explained by the model; the closer the R^2 value is to 1, the better the model fits the categorical differences of samples in the training set, and the more distinct the intergroup separation. Q^2 reflects the predictive ability of the model; a Q^2 value closer to 1 indicates better model predictive performance. ★ Selected principal component based on the largest Q^2.
Abbreviation: PLS-DA, Partial least squares discriminant analysis.

Characteristic Proteomic Perturbations in Elderly Sepsis

Thirteen DEPs specific to sepsis in the elderly were identified using four comparison groups: ES vs. EHC, YS vs. YHC, EHC vs. YHC, and ES vs. YS (Figure 9A). KEGG pathway enrichment analysis of these DEPs revealed eight significant biological pathways, including terpenoid backbone, cytokine-cytokine receptor interaction, and vitamin digestion (Figure 9B). These pathway enrichments were mainly driven by 5 proteins, including ZMPSTE24, CXCL14, INHBC, ATP6V1E1, and APOA1. These proteins and pathways constitute a distinct proteomic signature unique to elderly patients with sepsis, highlighting age-specific perturbations in immune regulation, energy metabolism, and nutrient homeostasis during a septic insult. The correlation between these proteins is shown in Figure 9C. Their levels in the EHC, YHC, ES, and YS groups are shown in Figure 9D.

Integrated Metabolomic and Proteomic Profiling Uncovers Characteristic Pathophysiological Alterations in Elderly Sepsis

To characterize the coordinated metabolic-proteomic regulatory network unique to ES patients, we performed a correlation analysis between 41 metabolites and 13 proteins specific to ES (Figure 10A), retaining pairs with a Spearman correlation coefficient of $|r_s| \geq 0.40$ for subsequent pathway enrichment and functional annotation (Figure 10B). Pathway analysis of the strongly correlated metabolites revealed three significantly perturbed pathways: D-amino acid metabolism; alanine, aspartate, and glutamate metabolism, and glycerophospholipid metabolism (Figure 10C). These pathway alterations were predominantly driven by two core metabolites, D-aspartic acid and LysoPC (18:1/0:0). Pathway analysis of the strongly correlated proteins identified 11 significantly enriched biological pathways, including terpenoid backbone biosynthesis, vitamin digestion and absorption, and collecting duct acid secretion (Figure 10D). To further annotate the biological functions of the correlated proteins, we performed GO enrichment analysis and identified the key processes, components, and functions driven by SCGB3A2, ATP6V1E1, APOA1, AP1G1, INHBC, CRYZL1, and CXCL14 (Figure 10E and Supplementary Material 2: sFigure 1).

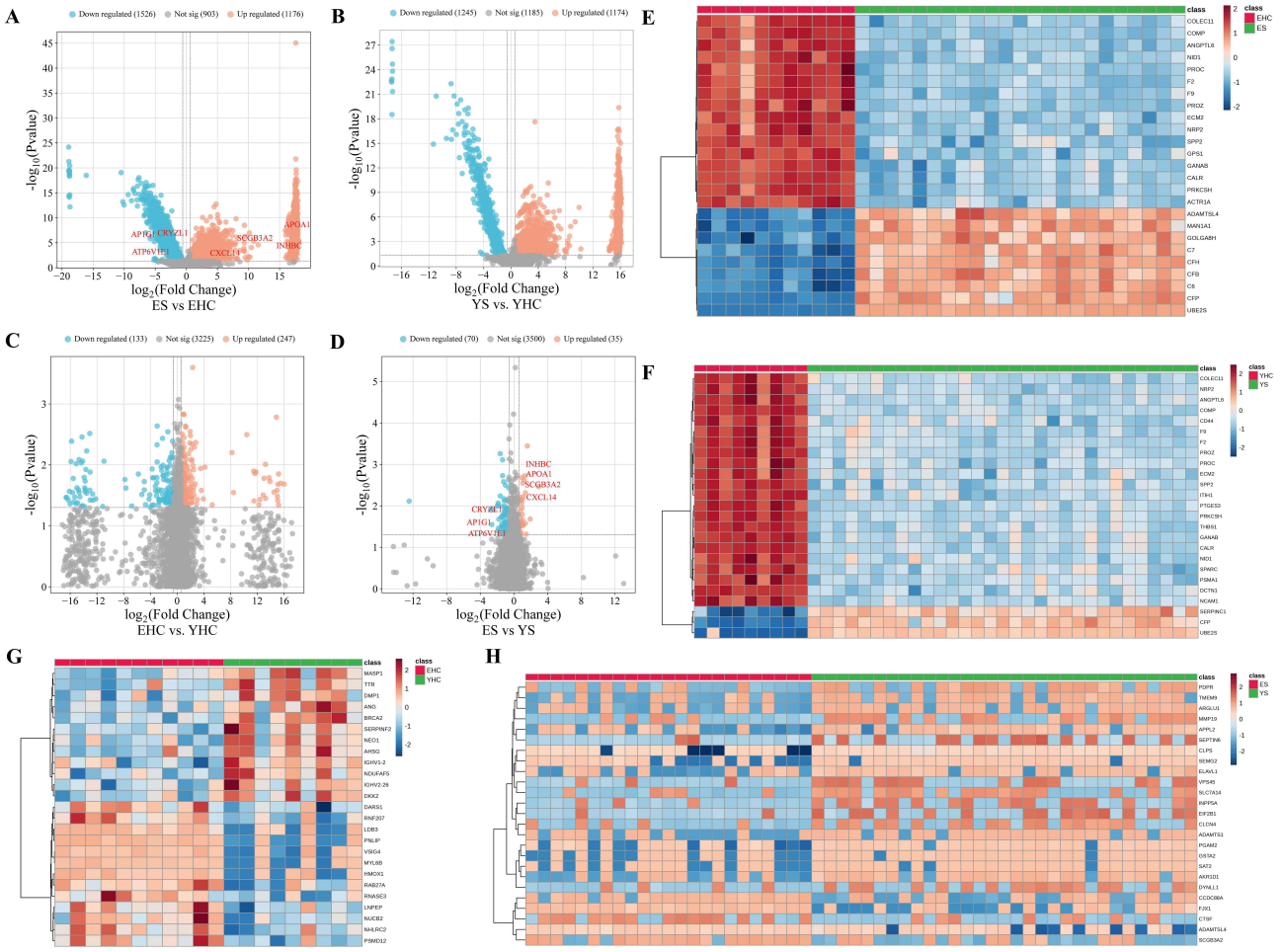

Figure 7 Volcano plot and Heatmap in proteomics. (**A**) Volcano plot in ES vs. EHC; (**B**) Volcano plot in YS vs. YHC; (**C**) Volcano plot in EHC vs.YHC; (**D**) Volcano plot in ES vs. YS; (**E**) Heatmap in ES vs. EHC; (**F**) Heatmap in YS vs. YHC; (**G**) Heatmap in EHC vs. YHC; (**H**) Heatmap in ES vs. YS.
Abbreviations: EHC, elderly healthy control; YHC, young healthy control; YS, young sepsis; ES, elderly sepsis.

Biological Process (BP)

The ketone metabolic process, regulation of intestinal cholesterol absorption, sterol import, cholesterol import, and positive regulation of lipoprotein lipase activity reflect profound disturbances in lipid and ketone body metabolism. Positive regulation of triglyceride lipase activity and negative regulation of heterotypic cell-cell adhesion highlighted altered lipolysis and cellular adhesion.

Cellular Component (CC)

The endocytic vesicle lumen indicates dysregulated endosomal trafficking. Other key components include proton-transporting V-type ATPase, V1 domain, vacuolar proton-transporting V-type ATPase complex, and multiple lipoprotein particles (low-density lipoprotein particles, chylomicrons, very-low-density lipoprotein particles, triglyceride-rich plasma lipoprotein particles), linking proton-driven ion transport and lipid transport compartments.

Molecular Function (MF)

Receptor ligand activity, signaling receptor activator activity, cytokine activity, and cytokine receptor binding reflect dysregulated immune and signaling molecule interactions. Ion transport and ATPase activity (ATPase-coupled ion transmembrane transporter activity, proton-transporting ATPase activity, rotational mechanism) and lipid binding (high-density lipoprotein particle binding, lipase inhibitor activity) further supported the functional roles of these proteins in ion homeostasis and lipid metabolism. The correlations between core hallmark metabolites and proteins in elderly patients with sepsis are presented in Table 2.

https://doi.org/10.2147/CIA.S613629

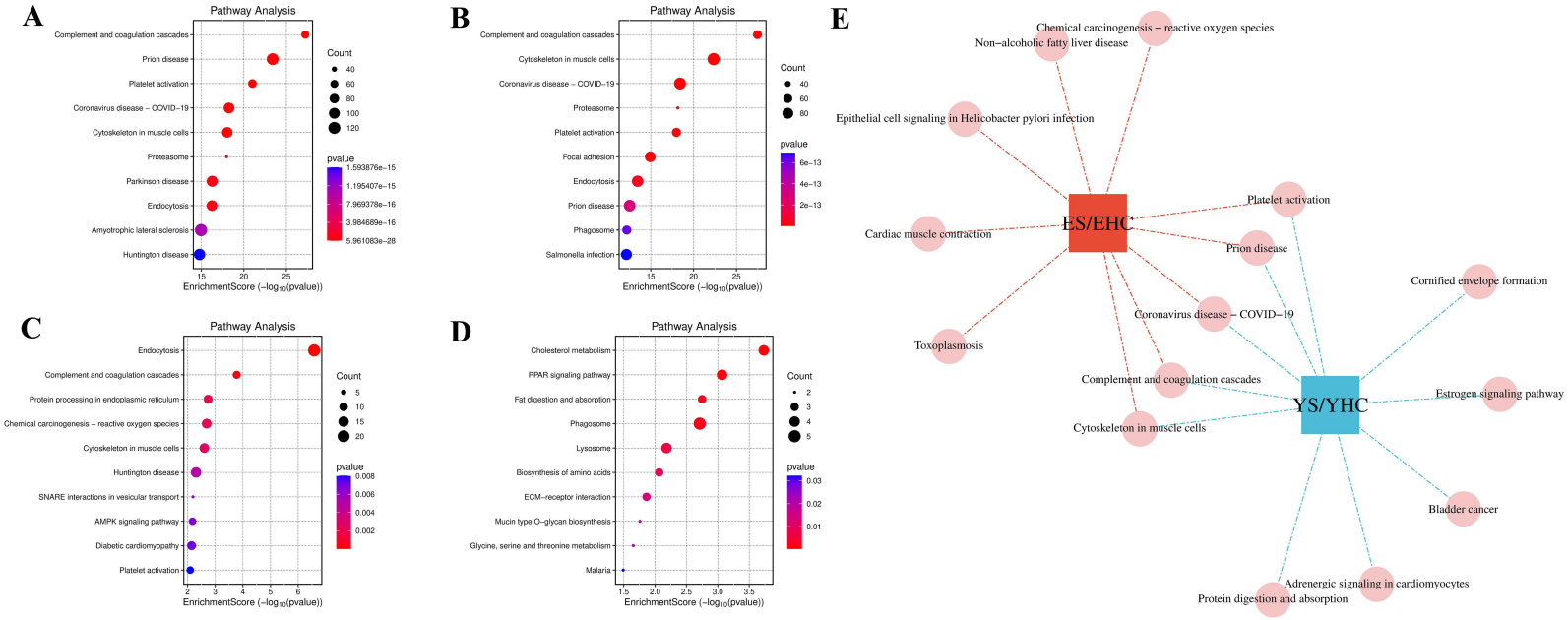

Figure 8 KEGG Enrichment analysis. (**A**) Top 10 proteomic pathways in ES vs. EHC; (**B**) Top 10 proteomic pathways in YS vs. YHC; (**C**) Top 10 proteomic pathways in EHC vs. YHC; (**D**) Top 10 proteomic pathways in ES vs. YS; (**E**) Co-enrichment network between elderly sepsis (ES vs. EHC) and young sepsis (YS vs. YHC).
Abbreviations: EHC, elderly healthy control; YHC, young healthy control; YS, young sepsis; ES, elderly sepsis.

https://doi.org/10.2147/CIA.S613629

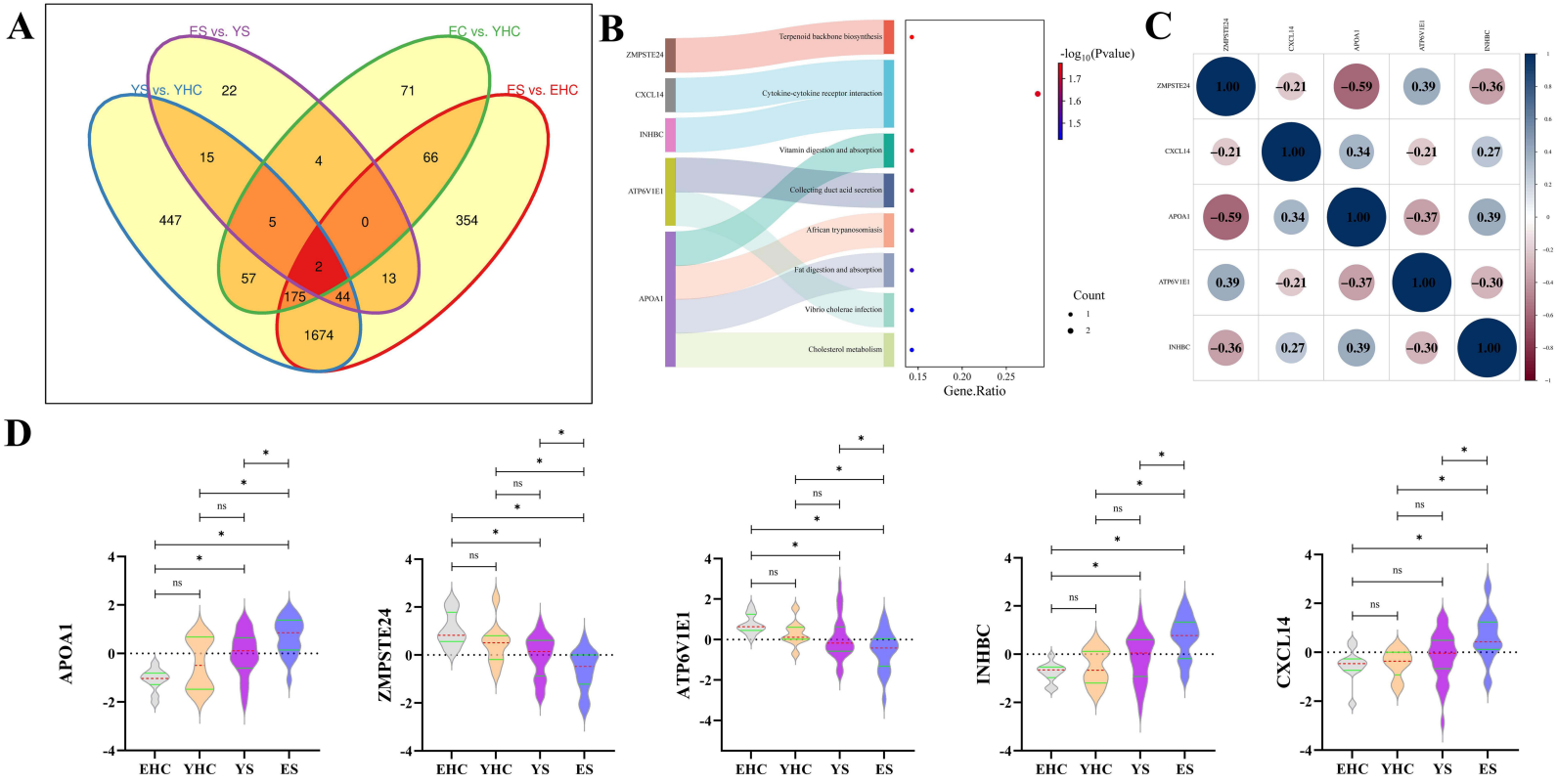

Figure 9 Characteristic proteomic perturbations in elderly sepsis. (**A**) Identification of differential metabolites specific to elderly sepsis; (**B**) KEGG enrichment analysis of DEPs specific to elderly sepsis; (**C**) Correlations analysis among DEPs enriched. (**D**) The levels of APOA1, ZMPSTE24, ATP6V1E1, INHBC, and CXCL14 in EHC, YHC, YS, and ES groups. *Statistically significant difference (P<0.05).
Abbreviations: EHC, elderly healthy control; YHC, young healthy control; YS, young sepsis; ES, elderly sepsis; ns, not significant.

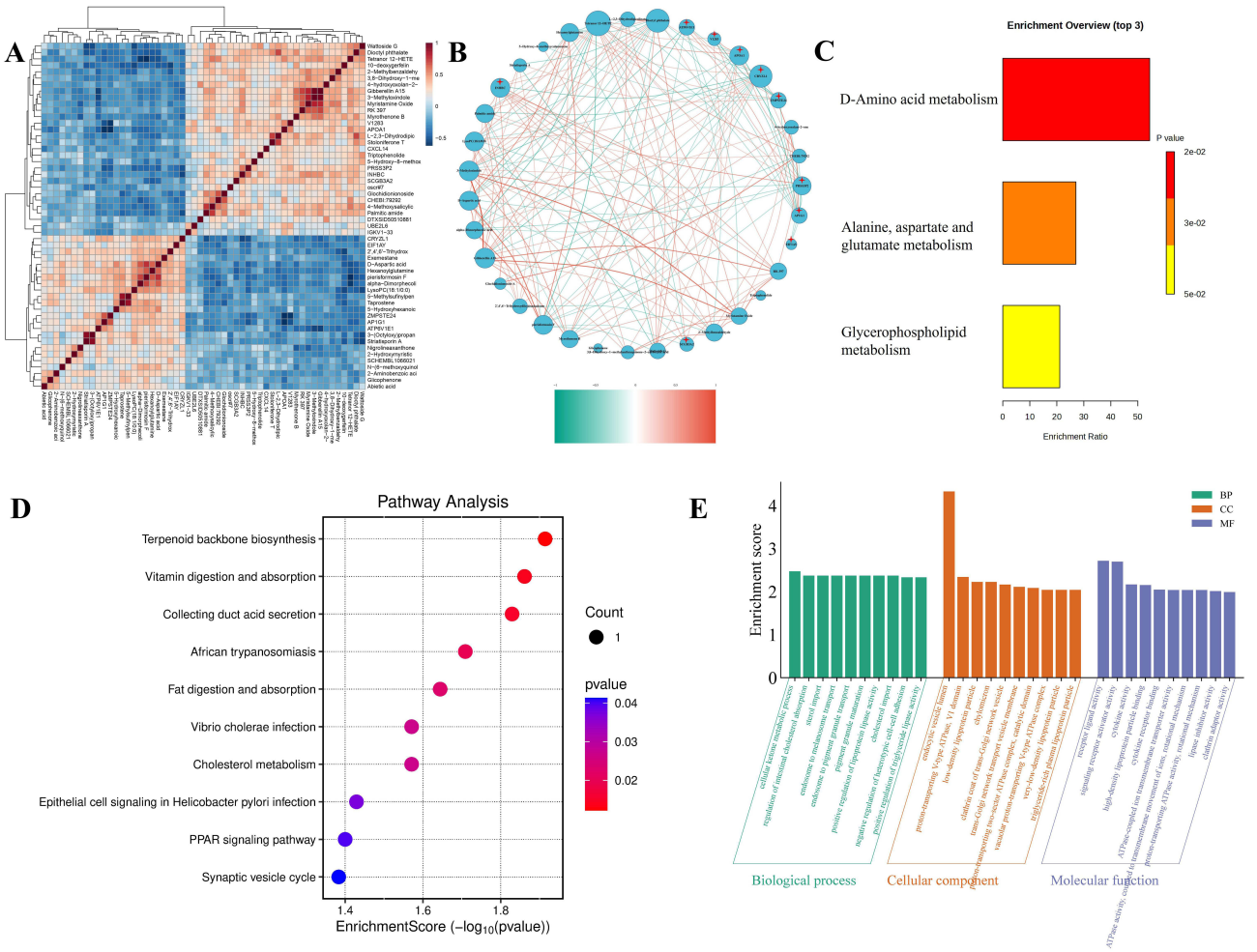

Figure 10 Integrated metabolomic and proteomic profiling uncovers characteristic pathophysiological Alterations in Elderly Sepsis. (**A**) Correlation analysis between the 41 metabolites and 13 proteins specific to elderly sepsis; (**B**) Correlation network of metabolites and proteins (|r| ≥ 0.4). (**C**) Pathway enrichment analysis of metabolites (|rs|≥ 0.4); (**D**) Pathway analysis of proteins (|rs|> 0.4); (**E**) GO Correlations between these metabolites and proteins enriched in metabolic and protein pathways; Annotation: Red four-pointed star represent proteins.

Discussion

In this study, we integrated metabolomics and proteomics to identify a coordinated network of metabolic and proteomic perturbations in ES, using a three-tiered screening strategy. These alterations are centered on dysregulated amino acid metabolism, disrupted lipid homeostasis, and aberrant immune-inflammatory signaling. The core hallmark metabolites and proteins include D-aspartic acid, LysoPC (18:1/0:0), SCGB3A2, ATP6V1E1, APOA1, AP1G1, INHBC, CRYZL1, and CXCL14, providing mechanistic insights into the unique pathophysiological vulnerabilities of elderly populations to septic insults.

Table 2 Correlations Between Core Hallmark Metabolites and Proteins in Elderly Sepsis

		ATP6V1E1	AP1G1	CRYZL1	SCGB3A2	INHBC	CXCL14	APOA1
D-Aspartic acid	r_s	0.142	0.376	0.423	−0.409	−0.259	−0.268	−0.296
	P	0.228	0.001	<0.001	<0.001	0.026	0.021	0.011
LysoPC(18:1/0:0)	r_s	0.369	0.390	0.460	−0.186	−0.333	−0.451	−0.422
	P	0.001	0.001	<0.001	0.112	0.037	0.004	<0.001

https://doi.org/10.2147/CIA.S613629

The adaptor protein complex 1 (AP1) subunit gamma-1 (AP1G1) encodes the γ1 subunit of AP-1 complex.[14] AP-1 is primarily localized in the trans-Golgi network. It is responsible for packaging cargo proteins bearing specific sorting signals into clathrin-coated vesicles and directing their transport to endosomes, lysosomes, or lysosome-related organelles.[14,15] AP1 contributes to the biogenesis of lysosome-related organelles and regulates the intracellular trafficking and degradation of immune receptors.[14–16] Compared with YS and HC, AP1G1 was significantly downregulated in ES. Its downregulation may lead to impaired phagolysosome maturation, preventing macrophages and neutrophils from efficiently delivering bacterial phagosomes to mature lysosomes, resulting in a reduced bactericidal capacity and persistent pathogens.[17–19] Impaired bactericidal function and sustained pathogen persistence in elderly septic patients may drive acute inflammation to become chronic, trigger repeated disease relapse, prolong hospital stay, and ultimately result in poor prognosis.[20–22] ATP6V1E1 encodes the E1 subunit of the V1 domain of the vacuolar-type ATPase (V-ATPase). V-ATPase is a multi-subunit rotary catalytic enzyme that uses energy from ATP hydrolysis to pump protons (H^+) across membranes into the organellar lumina or the extracellular space, thereby acidifying endosomes, lysosomes, and autolysosomes.[23,24] ATP6V1E1 is critical for regulating lysosomal acidification.[25] Its marked downregulation in elderly patients with sepsis impairs pathogen clearance by neutrophils and macrophages. Moreover, failure of autolysosomal acidification may block selective elimination of damaged mitochondria, triggering a cytokine storm followed by rapid immune paralysis. This may represent one of the underlying mechanisms explaining the impaired chemotaxis of neutrophils and the hyperinflammatory yet dysfunctional phenotype of monocytes and macrophages in elderly patients with sepsis, as observed by Lin et al[8] and Wanxue He[3] for single-cell sequencing studies. Collectively, the marked downregulation of AP1G1 and ATP6V1E1 may indicate impairment of the endosome-lysosome-autophagy axis in elderly patients with sepsis. Although reduced expression levels of AP1G1 and ATP6V1E1 were observed in the YS group, they were not significantly downregulated ($P < 0.05$, $2/3 < FC < 3/2$). Damage to this axis is particularly severe in ES, likely because aging is accompanied by decline in autophagic activity and lysosomal acidification capacity. Septic insult further suppresses AP1G1 and ATP6V1E1 expression, overwhelming cellular compensatory mechanisms and ultimately leading to the collapse of the endosome-lysosome-autophagy axis.

The above finding of disturbances in the endosome-lysosome-autophagy axis in ES patients was also validated by metabolomic analysis. Both D-aspartic acid and lysoPC (18:1/0:0) were positively correlated with AP1G1 and significantly downregulated in ES. D-aspartic acid is an endogenous d-amino acid that is widely distributed in mammalian tissues. It participates in regulating the intracellular redox status, inflammatory responses, and phagocytic activity.[26–28] Sara Falvo et al[26] reported that D-aspartic acid alleviated oxidative stress and apoptosis by activating the ERK/Akt/PCNA pathway. In D-Asp-treated TM4 cells, mitochondrial function and dynamics were enhanced, and endoplasmic reticulum stress was reduced. Xuechun Du et al[28] found that pre-treatment of human gingival fibroblasts with D-Asp for 24 h led to reduced cell membrane permeability and significantly decreased the expression of NLRP3, caspase-1, GSDMD, IL-1β, and IL-18. In ES, downregulation of D-aspartic acid may induce endoplasmic reticulum stress and mitochondrial dysfunction, thereby impairing lysosomal function. Lysophosphatidylcholine (LysoPC) interacts closely with lysosomes.[29–32] Chunyan Mu et al[29] reported that LysoPC disrupts the autolysosomal pathway and lysosomal acidification. The resultant osmotic imbalance across membranes leads to a loss of lysosomal integrity. The enhancement of lysosomal osmotic sensitivity causes lysosomes to become more susceptible to destabilization during osmotic shock. These results suggest that lysoPC plays a key role in phospholipase A2 (PLA2)-induced lysosomal destabilization. Albright et al[31] found that when lysosomal pH was elevated by pharmacological intervention, the activity of acid-dependent enzymes decreased, leading to reduced lysoPC levels. This revealed a direct causal relationship between the lysosomal functional status and lysoPC metabolism. Hyo-Ji Lee et al[32] also found that LPC enhanced phagosomal maturation in macrophages through the ROS-induced NF-κB signaling pathway. Collectively, the synchronous downregulation of the AP1G1 protein, LysoPC(18:1/0:0), and D-Asp indicates severe impairment of endosome-lysosome-autophagy in elderly patients with sepsis.

APOA1 is the most abundant protein component of high-density lipoprotein (HDL), accounting for approximately 70%, and is synthesized in the liver and small intestine.[33] APOA1 plays multiple protective roles in acute infection, including anti-inflammatory, vascular protective, antithrombotic, and immunomodulatory effects, which help the host resist infection, alleviate tissue damage, and maintain physiological homeostasis.[33,34] A decrease in its level is often

associated with greater infection severity and poor prognosis, whereas exogenous supplementation with APOA1 or HDL may hold therapeutic potential.[33,35] However, in our study, APOA1 was highly expressed in the ES tissues. Similar to our findings, Rashi Sehgal et al[36] also observed upregulation of proteins related to neutrophil activation and autophagy in sepsis, including APOA1. In ES, APOA1 is abnormally upregulated, but likely exists in a non-functional or hypofunctional form. This elevation may represent a failure of the body's compensatory response; the host attempts to compensate for functional defects by increasing synthesis yet fails to restore its protective effects. We also found that APOA1 was negatively correlated with LysoPC (18:1/0:0) ($r_s = -0.422$, $P < 0.001$). Highly concentrated, yet dysfunctional APOA1 may inhibit the activity of PLA2, resulting in decreased LysoPC, thereby linking the abnormal elevation of APOA1 to lysosome-related organelle dysfunction.

INHBC, also known as the inhibin βC chain, is a member of the transforming growth factor-β (TGF-β) superfamily. Wang et al[37] have linked it to the proliferation, migration, and invasion of hepatocellular carcinoma cells. However, research on INHBC in sepsis is limited. Only Liu et al,[38] based on plasma proteomics, found that INHBC is highly expressed in sepsis, and an enzyme-linked immunosorbent assay confirmed that its levels are significantly elevated in patients with sepsis To explore its function, we performed a correlation analysis between INHBC and inflammatory and immune factors and found that it was significantly correlated with a variety of such factors (Table 3). INHBC positively correlated with various potent pro-inflammatory factors, such as C3, C6, C9, and CXCL13, and negatively correlated with anti-inflammatory factors, including IL1RN. This indicates that INHBC exerts a strong proinflammatory effect, driving excessive inflammatory responses in ES. However, it also negatively correlated with CXCL8, suggesting that it may inhibit neutrophil migration and phagocytosis. Moderate inhibition of neutrophil migration may alleviate tissue damage, whereas excessive elevation of ES may compromise the ability of neutrophils to clear pathogens. These observations are consistent with previous single-cell studies showing impaired neutrophil chemotaxis in elderly patients with sepsis, alongside a hyperinflammatory but functionally defective phagocytic phenotype in monocytes and macrophages.[3,8] Collectively, INHBC play crucial roles in the inflammatory and immunomodulatory processes of ES. However, its role is complex, and extensive clinical and basic research is required to explore and validate its specific functions.

CXCL14 belongs to the chemokine CXC family. It attracts immune cells, such as monocytes and macrophages, to migrate toward sites of infection, helps initiate the host immune response, enhances the phagocytic capacity of macrophages and neutrophils, and promotes pathogen clearance.[39–41] Lai Xiaofei et al[40] found that the protein level of CXCL14 was significantly elevated in a mouse model of CLP-induced sepsis. Treatment with CXCL14 reduced mortality and improved bacterial clearance efficiency. Subsequent in vitro experiments further demonstrated that CXCL14 promotes phagosome formation in macrophages, thereby directly enhancing their bacterial phagocytosis and killing capacity. However, excessive upregulation of CXCL14 may be detrimental in elderly patients with sepsis. Although its upregulation can facilitate macrophage recruitment to infection sites and promote phagosome formation, collapse of the endosome–lysosome–autophagy axis in ES impairs the ability of macrophages to efficiently clear pathogens. Defective pathogen clearance triggers massive secretion of CXCL14, which recruits macrophages and ultimately culminates in tissue damage.

Collectively, by integrating metabolomics and proteomics with multiple screening strategies, we identified characteristic pathophysiological alterations in ES patients and proposed a hypothesis involving dysregulation of the endosome-lysosome-autophagy axis and immune-inflammatory imbalance (Figure 11). The physiological frailty inherent to sepsis in the elderly, combined with infection, leads to the downregulation of AP1, which suppresses the formation of clathrin-coated vesicles (CCVs) and impairs late endosome biogenesis, thereby blocking autolysosome formation. In

Table 3 INHBC Showed Significant Correlations with Inflammatory and Immune Factors ($R_s > 0.4$)

		C1QA	C1S	C1R	CXCL13	C3	C1QB	C9	IL6ST	C1QC
INHBC	r_s	0.573	0.572	0.550	0.538	0.510	0.502	0.496	0.490	0.488
	P	<0.001	<0.001	<0.001	<0.001	<0.001	<0.001	<0.001	<0.001	<0.001
		TNFRSF12A	SAA1	C6	SAA2	CXCL17	TNFRSF10C	TGFBI	CXCL8	IL1RN
INHBC	r_s	0.486	0.484	0.479	0.473	0.473	0.455	0.451	−0.503	−0.530
	P	<0.001	<0.001	<0.001	<0.001	<0.001	<0.001	<0.001	<0.001	<0.001

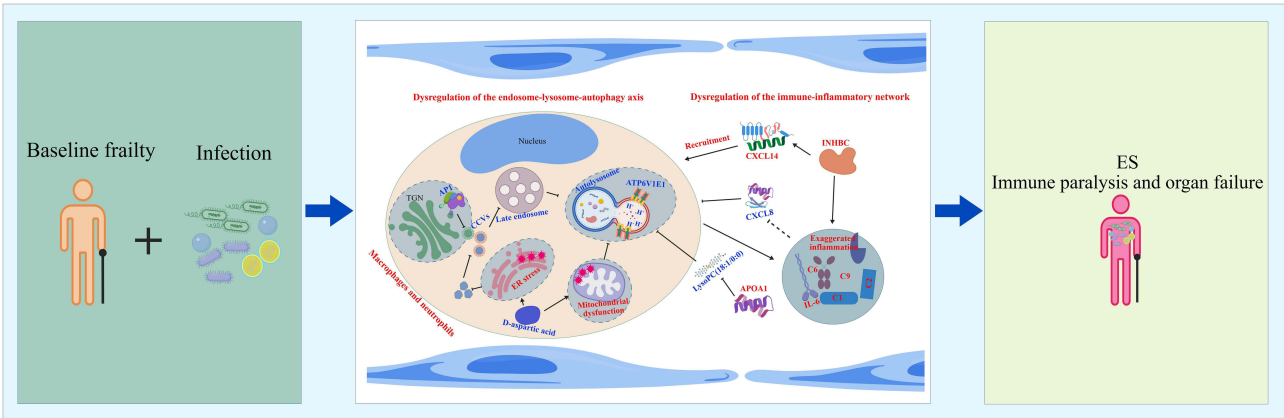

Figure 1 Hypothetical schematic of characteristic pathophysiological alterations in elderly sepsis. Red font indicates upregulation, blue font indicates downregulation, solid arrows represent promotion or induction, T-shaped lines (⊥) denote inhibition or blockage, and dashed T-shaped lines signify negative feedback inhibition. Created with BioGDP.com.[14]

Abbreviations: TGN, trans-Golgi network; CCVs, clathrin-coated vesicles; ER, endoplasmic reticulum; ES, elderly sepsis; AP1, Adaptor protein complex 1; ATP6V1E1, V-type proton ATPase subunit E 1; CXCL14, C-X-C motif chemokine 14; INHBC, Inhibin beta C chain; CXCL8, C-X-C motif chemokine 8; APOA1, Apolipoprotein A-I.

addition, reduced levels of D-aspartic acid trigger endoplasmic reticulum stress, which in turn inhibits protein and lipid synthesis and compromises CCV biogenesis, ultimately impairing autolysosome formation. Decreased D-aspartic acid also causes mitochondrial dysfunction, impairs ATP synthesis, inhibits V-ATPase activity, and hinders lysosomal acidification. Furthermore, the downregulation of ATP6V1E1 also contributes to defective lysosomal acidification. Defects in autolysosome formation and lysosomal acidification reduce the ability of neutrophils and macrophages to clear pathogens and damaged mitochondria, thereby exacerbating the inflammatory response. Meanwhile, upregulation of INHBC stimulates excessive secretion of various cytokines and inflammatory mediators, leading to an overexuberant inflammatory response. It also upregulates CXCL14 expression, recruiting large numbers of functionally impaired neutrophils and macrophages and further amplifies inflammation. Such excessive inflammation induces a negative feedback inhibition of CXCL8 expression, reducing the recruitment of inflammatory cells. This cascade ultimately results in immune paralysis and multiple organ injury.

A multicenter study by Güngör et al[42] revealed that elderly critically ill patients generally suffer from a triple burden of advanced age, multiple comorbidities, and a high incidence of sepsis. Clinically, it has long puzzled clinician why elderly patients exhibit more dysregulated inflammatory responses, more persistent organ damage, and a more difficult recovery process when confronted with similar pathogenic insults. Our findings provide a mechanistic theoretical basis for this clinical dilemma. In elderly sepsis patients, the downregulation of AP1G1 and ATP6V1E1 marks impaired lysosomal acidification and sorting function, and the concomitant depletion of D-aspartic acid and LysoPC further confirms the dysfunction of the endosome–lysosome–autophagy axis. Severe impairment of intracellular clearance leads to uncontrolled inflammatory recruitment signals driven by INHBC and CXCL14. A large number of recruited phagocytes fail to exert effective bactericidal activity due to intrinsic defects in their degradation capacity, ultimately shifting the protective immune response toward immune paralysis and sustained tissue injury. Consistent with previous research by Baykara et al[43], mortality in critically ill patients is strongly linked to organ dysfunction and inflammatory burden. Accordingly, the disrupted endosome–lysosome–autophagy axis and immune-inflammatory homeostasis observed in our study may contribute to poor clinical outcomes in ES. Therefore, targeted evaluation and intervention of the endosome–lysosome–autophagy axis hold great promise for optimizing and reshaping the diagnosis and treatment landscape of ES. Collectively, these findings hold considerable translational potential for clinical practice in ES. The synchronous downregulation of AP1G1, ATP6V1E1, D-aspartic acid, and LysoPC(18:1/0:0) constitutes a molecular signature of endosome–lysosome–autophagy axis collapse that may serve as an early prognostic tool to identify patients at highest risk of persistent organ dysfunction and secondary infections. Meanwhile, the divergent expression patterns of APOA1, INHBC, CXCL14, and SCGB3A2 offer a framework for bedside immunophenotyping: an elevated INHBC and CXCL14 ratio may flag a hyperinflammatory yet immunoparalytic state requiring restrained immunomodulation, whereas

https://doi.org/10.2147/CIA.S613629

profound SCGB3A2 depletion may indicate epithelial barrier failure amenable to reparative strategies. Together, these biomarkers could be integrated into a sequential two-step clinical algorithm—diagnostic triage followed by prognostic stratification—to promote the development of elderly sepsis management toward mechanism-driven and precision-targeted intervention.

However, this study had several limitations. First, this was a single-center study that may have been subject to selection bias, and the sample characteristics may not be representative of the broader ES population, thereby limiting the generalizability of the findings. Second, as an exploratory study, it lacked validation in a multicenter cohort and did not involve in vivo or in vitro experiments to elucidate specific underlying mechanisms. Third, the sample size was limited. Although permutation tests indicated no overfitting of the PLS-DA model, the small sample size may have compromised the reproducibility and reliability of the results. Fourth, the omics data were not directly correlated with established clinical severity scores such as SOFA or APACHE II, which limits our ability to quantitatively link molecular alterations with bedside assessments of organ dysfunction and illness severity. Fifth, all analyses were performed on samples collected at a single time point in a cross-sectional design, precluding causal inferences regarding the relationship between the identified molecular disturbances and clinical outcomes. Sixth, the study lacks an independent prospective validation cohort; whether the key molecules identified here can reliably predict clinical trajectories or guide therapeutic decisions remains to be tested in longitudinal, multicenter studies. Future multicenter clinical studies are needed to validate these findings. Additionally, in vivo and in vitro experiments are needed to explore the specific functions of these characteristic metabolites and proteins as well as their impact on the prognosis of elderly patients with sepsis.

Conclusion

Despite these limitations, this study is the first to integrate metabolomics and proteomics via an innovative multistep screening approach to explore the characteristic pathophysiological alterations in ES and propose the hypothesis of dysregulation of the endosome-lysosome-autophagy axis and immune-inflammatory imbalance, which provides a theoretical basis for further exploring the pathophysiological mechanism of ES and developing precise therapeutic strategies.

Abbreviations

ES elderly sepsis, CLP cecal ligation and puncture, EHC elderly healthy control, YS young sepsis, YHC young healthy controls, PLS-DA partial least squares discriminant analysis, FC fold-change, VIP variable importance in projection, DEMs differentially expressed metabolite, DEP differentially expressed protein, SOFA sequential organ failure assessment, KEGG Kyoto Encyclopedia of Genes and Genomes, GO Gene Ontology, ANC absolute neutrophil count, AMC absolute monocyte count, AP1 Adaptor protein complex 1, V-ATPase vacuolar-type ATPase, LysoPC Lysophosphatidylcholine.

Data Sharing Statement

Data are available upon request from Jianzhong Yang (Email: yjz6542@126.com).

Funding

This study was supported by grants from the National Natural Science Foundation of China (82260379), the In-hospital Program for the Cultivation of Excellent Talents and Innovative Teams of the First Affiliated Hospital of Xinjiang Medical University (cxtd202408), and the 2025 Young Researchers' Scientific Research Launch Program at the First Affiliated Hospital of Xinjiang Medical University (2025YFY-QKQN-12).

Disclosure

The authors declare that they have no known competing financial interests or personal relationships that could have appeared to influence the work reported in this paper.

References

1. Singer M, Deutschman CS, Seymour CW, et al. The third international consensus definitions for sepsis and septic shock (Sepsis-3). *JAMA*. 2016;315 (8):801. doi:10.1001/jama.2016.0287

2. Cai J, Jin Y, Lou J, et al. The V-shaped association between the ratio of neutrophil counts to prognostic nutritional index and 30-, 60-, and 90-day mortality in elderly critically ill patients aged 65 and older with sepsis: a retrospective study based on the MIMIC database. *Front Nutr*. 2025;12:1602016. doi:10.3389/fnut.2025.1602016
3. He W, Yao C, Wang K, et al. Single-cell landscape of immunological responses in elderly patients with sepsis. *Immun Ageing*. 2024;21(1):40. doi:10.1186/s12979-024-00446-z
4. Huang C, Gou Y, Cong Y, et al. Metabolomics reveals glyoxylate and dicarboxylate metabolism disorder in elderly trauma: a Retrospective Study. *Clin Interventions Aging*. 2049–2064;2025(20). doi:10.2147/CIA.S552626
5. Zhu X, Li W, Lv Z, et al. Integration of metabolic parameters with SOFA score for mortality risk assessment in elderly sepsis: a derivation study. *BMC Infect Dis*. 2025;25(1):1596. doi:10.1186/s12879-025-12031-w
6. Zhu XY, Jiang ZM, Li X, et al. Interpretive machine learning predicts short-term mortality risk in elderly sepsis patients. *Front Physiol*. 2025;16:1549138. doi:10.3389/fphys.2025.1549138
7. Zhang L, Liu H, Zhang D, et al. Non-linear association between lactate and 28 days mortality in elderly patients with sepsis across different SOFA score groups: results from the eICU Collaborative Research Database. *Front Med*. 2025;12:1605319. doi:10.3389/fmed.2025.1605319
8. Lin Y, Zhou Z, Yang M, et al. Single-cell transcriptomic analysis reveals immune remodeling in bone marrow during aged sepsis. *Geroscience*. 2025. doi:10.1007/s11357-025-01966-2
9. Wu HQ, Gou Y, Li DD, et al. Revealing protein profiles and pathways in elderly trauma patients based on plasma proteomics. *J Surg Res*. 2026;321:274–284. doi:10.1016/j.jss.2026.03.002
10. Xu D, Liao S, Li P, et al. Metabolomics coupled with transcriptomics approach deciphering age relevance in sepsis. *Aging and Disease*. 2019;10 (4):854. doi:10.14336/AD.2018.1027
11. Gou Y, Lv BH, Zhang JF, et al. Identifying early predictive and diagnostic biomarkers and exploring metabolic pathways for sepsis after trauma based on an untargeted metabolomics approach. *Sci Rep*. 2025;15(1):12068. doi:10.1038/s41598-025-92631-3
12. Chen Q, Liang X, Wu T, et al. Integrative analysis of metabolomics and proteomics reveals amino acid metabolism disorder in sepsis. *J Transl Med*. 2022;20(1):123. doi:10.1186/s12967-022-03320-y
13. Gou Y, dan LD, Li X, et al. Integrated metabolomics and proteomics to screen early diagnostic biomarkers of venous thromboembolism following severe trauma: a retrospective study. *Injury*. 2026;57(2):112934. doi:10.1016/j.injury.2025.112934
14. Liu Y, Xu P, Rivara S, et al. Clathrin-associated AP-1 controls termination of STING signalling. *Nature*. 2022;610(7933):761–767. doi:10.1038/s41586-022-05354-0
15. Liu Y, Li F, Wu B, et al. The clathrin adaptor AP1-S1 is associated with immune infiltration and HLA loss, as a potential therapeutic target in lung adenocarcinoma. *Int Immunopharmacol*. 2025;152:114385. doi:10.1016/j.intimp.2025.114385
16. Silva L. CD4 down-regulation by HIV-1 Nef reveals distinct roles for γ1 and γ2 subunits of AP-1 complex in protein trafficking. *J Cell Sci*. 2017;130(2):429–443. doi:10.1242/jcs.192104
17. Zotta A, Toller-Kawahisa J, Palsson-McDermott EM, et al. Mitochondrial respiratory complex III sustains IL-10 production in activated macrophages and promotes tumor-mediated immune evasion. *Sci Adv*. 2025;11(4):eadq7307. doi:10.1126/sciadv.adq7307
18. Hackert NS, Radtke FA, Exner T, et al. Human and mouse neutrophils share core transcriptional programs in both homeostatic and inflamed contexts. *Nat Commun*. 2023;14(1):8133. doi:10.1038/s41467-023-43573-9
19. Jegga AG, Schneider L, Ouyang X, et al. Systems biology of the autophagy-lysosomal pathway. *Autophagy*. 2011;7(5):477–489. doi:10.4161/auto.7.5.14811
20. Wan Muhd Shukeri WF, Mat Nor MB, Md Ralib A. Sepsis and its impact on outcomes in elderly patients admitted to a Malaysian intensive care unit. *Malays J Med Sci*. 2022;29(3):145–150. doi:10.21315/mjms2022.29.3.14
21. Mankowski RT, Anton SD, Ghita GL, et al. Older sepsis survivors suffer persistent disability burden and poor long-term survival. *J American Geriatrics Society*. 2020;68(9):1962–1969. doi:10.1111/jgs.16435
22. Xu C, Lv L, Hu W, et al. Long-Term outcomes in older patients with sepsis in the ICU: a Retrospective Study. *Altern Ther Health Med*. 2024;30 (2):124–130.
23. Yu H, Chen J, Wang F, et al. Capsaicin alleviates autophagy-lysosomal dysfunction via PPARA-Mediated V-ATPase subunit ATP6V0E1 signaling in 3xTg-AD mice. *Adv Sci*. 2025;12(39):e02707. doi:10.1002/advs.202502707
24. Zhan Y, Deng C, Tang L, et al. NAT10 increases lysosomal acidification to promote esophageal cancer metastasis via ac4C acetylation of ATP6V0E1 mRNA. *Adv Sci*. 2025;12(31):e02931. doi:10.1002/advs.202502931
25. Chen J. Mycobacterium tuberculosis modulates phosphorylation of host ATP6V1E1 to promote intracellular survival. *Nature Communications*. 2026.
26. Falvo S, Grillo G, Latino D, et al. Potential role of mitochondria and endoplasmic reticulum in the response elicited by D-aspartate in TM4 Sertoli cells. *Front Cell Dev Biol*. 2024;12:1438231. doi:10.3389/fcell.2024.1438231
27. Kinouchi T, Matsuda A, Kawakami S, et al. Influence of oxidative stress on D -aspartyl endopeptidase activity. *Chem Biodivers*. 2010;7 (6):1398–1402. doi:10.1002/cbdv.200900345
28. Du X, Li B, Cai Q, et al. D-aspartic acid protects against gingival fibroblasts inflammation by suppressing pyroptosis. *Mol Biol Rep*. 2022;49 (7):5821–5829. doi:10.1007/s11033-022-07335-y
29. Mu C, Shao K, Su M, et al. Lysophosphatidylcholine promoting α-Synuclein aggregation in Parkinson's disease: disrupting GCase glycosylation and lysosomal α-Synuclein degradation. *npj Parkinsons Dis*. 2025;11(1):47. doi:10.1038/s41531-025-00902-7
30. Hu JS, Li YB, Wang JW, Sun L, Zhang GJ. Mechanism of lysophosphatidylcholine-induced lysosome destabilization. *J Membrane Biol*. 2007;215 (1):27–35. doi:10.1007/s00232-007-9002-7
31. Albright JM, Sydor MJ, Shannahan J, et al. Imipramine treatment alters sphingomyelin, cholesterol, and glycerophospholipid metabolism in isolated macrophage lysosomes. *Biomolecules*. 2023;13(12):1732. doi:10.3390/biom13121732
32. Lee HJ, Hong WG, Woo Y, et al. Lysophosphatidylcholine enhances bactericidal activity by promoting phagosome maturation via the activation of the NF-κB pathway during salmonella infection in mouse macrophages. *Mol Cells*. 2020;43(12):989–1001. doi:10.14348/molcells.2020.0030
33. Guo K, Hu C, Li L, et al. ApoA1/HDL and sepsis-associated vascular endothelial injury: a narrative review. *Crit Care*. 2025;29(1):426. doi:10.1186/s13054-025-05668-1

34. Rosanaly S, Apalama ML, Bringart M, et al. Production, characterization and biodistribution of therapeutic high-density lipoprotein-like nanoparticles reconstituted with or without histidine-tagged recombinant ApoA1. *Biochimica et Biophysica Acta BBA*. 2025;1870(3):159606. doi:10.1016/j.bbalip.2025.159606
35. Bulgarelli C, Ciuffoli E, Troia R, et al. Apolipoprotein A1 and serum amyloid A in dogs with sepsis and septic shock. *Front Vet Sci*. 2023;10:1098322. doi:10.3389/fvets.2023.1098322
36. Sehgal R, Kaur N, Maiwall R, et al. Plasma proteomic analysis identified proteins associated with faulty neutrophils functionality in decompensated cirrhosis patients with sepsis. *Cells*. 2022;11(11):1745. doi:10.3390/cells11111745
37. Wang H, Hu K, Tang C, et al. Identification of causal plasma proteins and targeted therapy for primary hepatic carcinoma via proteome-wide Mendelian randomization. *Commun Biol*. 2025;8(1):1849. doi:10.1038/s42003-025-09274-3
38. Liu B, Jin Y, Ding Y, Gu Y, Zhou J, Luo C. Therapeutic targets for sepsis: multicenter proteome-wide analyses and experimental validation. *J Proteome Res*. 2025;24(7):3498–3506. doi:10.1021/acs.jproteome.5c00148
39. Korbecki J, Kojder K, Kapczuk P, et al. The effect of hypoxia on the expression of CXC chemokines and CXC chemokine receptors—a review of literature. *IJMS*. 2021;22(2):843. doi:10.3390/ijms22020843
40. Lai X, Ding H, Yu R, et al. CXCL14 protects against polymicrobial sepsis by enhancing antibacterial functions of macrophages. *Am J Respir Cell Mol Biol*. 2022;67(5):589–601. doi:10.1165/rcmb.2022-0249OC
41. Tsujihana K, Tanegashima K, Santo Y, et al. Circadian protection against bacterial skin infection by epidermal CXCL14-mediated innate immunity. *Proc Natl Acad Sci USA*. 2022;119(25):e2116027119. doi:10.1073/pnas.2116027119
42. Güngör S, Ediboğlu Ö, Yazıcıoğlu Moçin Ö, et al. Evaluation of patients with COVID-19 followed up in intensive care units in the second year of the pandemic: a multicenter point prevalence study. *Thorac Res Pract*. 2023;25(1):11–16. doi:10.5152/ThoracResPract.2023.23024
43. Baykara N. PREGCOVID-ICU study group. clinical characteristics, outcomes, and risk factors for mortality in pregnant/puerperal women with COVID-19 admitted to ICU in Turkey: a multicenter, retrospective study from a middle-income country. *J Intensive Care Med*. 2024;39(6):577–594. doi:10.1177/08850666231222838